Acta Polytechnica **66**(2):196–208, 2026
https://doi.org/10.14311/AP.2026.66.0196

Published by the Czech Technical University in Prague

SILICA SAND SUBSTITUTES IN AUTOCLAVED AERATED CONCRETE: UTILISATION OF SECONDARY RAW MATERIALS

Lenka Mészárosová[a,*], Vít Černý[a], Jindřich Melichar[a], Jakub Hodul[a], Winfried Malorny[b], Rostislav Drochytka[a]

[a] *Brno University of Technology, Faculty of Civil Engineering, Veveří 95, 602 00 Brno, Czech Republic*

[b] *University of Applied Sciences technology, Business and Design, Faculty of Engineering, Ph.-Müller-Straße, 23966 Wismar, Germany*

[*] corresponding author: lenka.meszarosova@vut.cz

Abstract. This article provides an in-depth analysis of the use of non-traditional secondary raw materials as a partial replacement for silica sand in the autoclaved aerated concrete (AAC). Three types of foundry sand from different sources and three varieties of waste glass (WG) were selected and subjected to experimental evaluation at substitution levels of 5 %, 10 %, and 15 %. The experimental verification reveals that using foundry sand and WG results in physico-mechanical and mineralogical properties comparable to, and in certain cases superior to, conventional AAC formulations. Conversely, brown and mixed WG led to the formation of atypical mineral phases, which significantly influenced the characteristics of AAC. Of the evaluated materials, foundry sand sourced from non-ferrous casting operations emerged as the most promising alternative, particularly at a 10 % substitution, where enhanced strength and an optimised microstructure were observed. The article presents a structured experimental methodology, segmented into three stages: the selection and preparation of secondary raw materials, a comprehensive assessment of their physico-mechanical properties, and an advanced microstructural characterisation. The findings underscore the feasibility of using these secondary raw materials in AAC manufacturing without compromising material performance.

Keywords: Autoclaved aerated concrete, waste foundry sand, waste glass.

1. Introduction

Autoclaved aerated concrete (AAC), as one of the key building materials, is usually prepared as a mixture of highly pure materials: siliceous component (mostly silica sand), lime, Portland cement, aerating agent, and other admixtures [1, 2]. Generally, the dry bulk density of AAC lies within the range of 200–1000 kg m^{-3}. The compressive strength of AAC increases with density and values range from 1 to 9 MPa [3, 4]. The strength of the final product is achieved primarily through the hydrothermal treatment during the autoclaving process [5]. Autoclaving is a process that produces various calcium hydro silicates with molar ratios of $CaO:SiO_2$ ranging from 0.5 to 3.0 with varying amounts of crystal-bound water due to hydrothermal reactions. The most important mineral present is tobermorite, which has the chemical formula $Ca_4[Si_6O_{18}H_2] \cdot Ca \cdot 4H_2O$, abbreviated to $C_5S_6H_5$. It forms plate-like (leaf-like) or lath-like crystals in a rhombic crystallographic system and is a strength carrier [6]. The formation of the solid macrostructure is strongly influenced by the solubility of β-silica, silica gel, and $Ca(OH)_2$ in water as the hydrothermal synthesis takes place in the liquid phase. The solubility of $Ca(OH)_2$ decreases as a function of temperature, whereas the solubility of SiO_2 increases with increasing temperature. The intersection of the solubility curves of β-silica and $Ca(OH)_2$ for tobermorite formation corresponds to a temperature between 174 and 193 °C, with a corresponding pressure of 0.8 to 1.3 MPa. The progress and time of autoclaving depend on the conditions of tobermorite formation, which are dependent on the properties of the starting materials, such as chemical nature, specific surface, $CaO:SiO_2$ ratio, amount of admixture water, and types and amounts of impurities. The onset of its formation is indicated after about 8 hours of autoclaving. A significantly longer autoclaving time (20 to 72 hours) produces xonotlite, which has significantly poorer strength characteristics than tobermorite [2, 7].

Recent studies have explored the possibility of utilising various waste products in AAC production, demonstrating the feasibility of incorporating diverse waste materials, offering environmental benefits and potentially improving the characteristics of the final product. Various industrial wastes, such as fly ash and marble slurry, have been explored as partial replacements for traditional raw materials such as sand [8]. These substitutions can improve AAC's physico-mechanical properties, including density, compressive strength, and water absorption [9]. Utilising waste materials in AAC production not only addresses environmental concerns but also contributes to sustainable construction practices.

However, there are still challenges in the recycling of AAC waste from construction sites [10]. Some studies

describe successfully utilising concrete slurry waste (a pollutant from the ready-mixed concrete industry) in AAC at high contents of up to 60 %, with the addition of nano-silica and silica fume improving mechanical properties [11]. Fine fractions of processed waste concrete and sorted construction waste have also shown potential as quartz sand substitutes in AAC, helping to conserve natural resources [12]. Furthermore, waste from gas cleaning of industrial waste combustion has been investigated as a partial lime replacement in AAC production. This waste enhanced mechanical properties and influenced pore size distribution, while also potentially reducing CO_2 emissions due to its high CaO content [13].

Among the various secondary raw materials explored for AAC production, waste glass has recently gained increased attention due to its chemical composition and availability. When used as a partial replacement of aggregate, waste glass can significantly influence the properties of AAC. Traditional concrete properties can be negatively affected by WG presence, including compressive strength and air content, while also contributing to alkali-silica reactions [14]. When incorporated as a replacement for silica in AAC mixtures, WG can improve compressive strength, with optimal results achieved at 20 % replacement rate [15]. Adding WG to AAC can also lead to decreased porosity and water absorption, while increasing bulk density, thermal conductivity, and ultrasonic wave velocity [16]. When used as a partial cement replacement, finely ground WG can enhance compressive strength properties, with the level of replacement and particle size distribution being crucial factors [17]. According to the statistical yearbook of the Ministry of the Environment, more than 40 thousand tonnes of waste packaging glass with the code 15 01 07 Glass packaging, 9 169 tonnes of glass construction and demolition waste with the code 17 02 02 Glass, and 162 403 tonnes of glass waste from separate collection with the waste code 20 01 02 Glass have been produced annually in recent years [18]. The glass waste generated is mainly used to create new glass products, i.e. it is recycled in a small circle. The substitution of primary raw materials used in the glass industry saves natural resources of sand, limestone, feldspars, etc. Due to its high SiO_2 content, glass recyclate could be used as a substitute for silica sand in building materials.

Furthermore, fibre-like secondary raw materials have shown a potential to improve physical-mechanical properties of AAC [19]. Short glass fibres can influence the initial suspension, foaming behaviour, and strength characteristics, with fibre orientation and concentration playing crucial roles [20]. Additionally, the partial replacement of siliceous components with various fibres, such as basalt, rice husk, and granite, has been studied in order to enhance mechanical and physical properties while addressing waste management issues [21]. These advancements in utilising fibre are expanding the applications of AAC in construction.

Waste foundry sand (WFS) has already been explored as a sustainable alternative to natural sand in traditional concrete production. WFS is produced during the casting of molten metal into a casting mould prepared from a moulding compound. During this process, the sand acquires a black colour. High-quality sand can be recycled by regeneration, but material reuse has its limits. If recycling is not possible or is not performed, the sand becomes waste [22]. Approximately 800 000 tonnes of foundry sand (mostly silica sand with suitable properties for use in the foundry industry) are used per year to make moulding compounds for foundries. Less than 10 % is returned to circulation through the regeneration process. Used casting moulds that have not been reclaimed remain unused and account for approximately 70 % of foundry waste, which is approximately 2 % of the total waste generated in the Czech Republic [23]. Studies have shown that replacing up to 20–40 % of fine aggregate with WFS can enhance the mechanical strength and durability properties of concrete [24, 25]. However, higher replacement levels can reduce workability [22]. The use of WFS in concrete production offers environmental benefits by reducing natural sand extraction and addressing waste disposal issues [26]. WFS, a byproduct of metal casting industries, contains high silica content, making it suitable for various civil engineering applications [27]. While most studies report positive outcomes, some cases have shown reduced material properties when using WFS [26]. WFS in dosages 20 %, 40 %, and 60 % was also tested as a possible replacement of silica component in non-AAC. Authors of this study concluded that the optimal dosage of WFS is 20 % [28]. The comparison of the influence of different alternative siliceous components (WFS and WG) on physico-mechanical parameters of AAC prepared in otherwise same conditions is not sufficiently described yet. The hypothesis is that some amounts of these waste materials can positively impact the properties of AAC.

2. Materials and methods

2.1. Materials characterisation

The materials used to prepare the AAC samples were lime, cement, and calcium sulphate as the binding mixture. Basic properties of input raw materials are stated in Tables 1–5.

In terms of siliceous components, silica sand was partially replaced with foundry sand and WG. Properties of samples with three types of foundry sand with different chemical compositions were compared with samples containing the three types of WG from separate collections. The WG came from separate collections of different colours and purities, classified according to the Czech legislation under the waste catalogue as group 20 “Municipal waste” (household and similar trade waste, industrial waste, and waste from authorities) including components from separate

Oxides	CaO + MgO	MgO	SiO_2	Fe_2O_3	Al_2O_3	SO_3	CO_2	CaO free
Content [%]	93.00	0.58	0.54	0.13	0.23	0.35	3.89	85.70

Table 1. Chemical composition of CL 90-Q V7 lime.

Properties	Units	Values
Residua on 0.2 mm mesh	%	0.08
Residua on 0.090 mm mesh	%	5.88
Reactivity t_{60}	minutes	7.5
Tapped density	$kg\,m^{-3}$	915

Table 2. Physical properties of CL 90-Q V7 white lime.

Compound	Content in %
Clinker	90.61
Limestone	6.31
SO_3	2.39
Cl-	0.04
Na_2O	0.65

Table 3. Composition of CEM II/A-LL 52.5 R.

collections under the group 20 01 and components from separate collections under the group 20 01 02 "Glass" [29].

A lime of the CL 90 class with a reactivity of R5 and a grain size of P1 according to EN 459-1 [30], which meets the conditions for use in the production of aerated concrete, was used.

Silica sand with a content of more than 70 % of silica dioxide was used as the siliceous component. The siliceous component was milled to a fineness of about $2\,600\,cm^2\,g^{-1}$ using a ball mill, in order to achieve a comparable particle size distribution for all the materials used. The particle sizes of the secondary raw materials used are shown in comparison with the reference material in Figures 1 and 2.

This raw material was partially replaced at three different rates (5 %, 10 % and 15 %) with a potentially suitable waste material (WFS and WG). Then it was mixed with water and tempered to a temperature of 45 °C before mixing.

Aluminium powder with a fineness of 88.1 % and a subsieve fraction of 90 µm was used as the aerating agent. Recycled return slurry sludge (RRS) was used to better simulate real production conditions and the objectivity of using non-traditional secondary raw materials in production. The flue-gas desulphurisation gypsum (FGDG) with a purity of 92–96 % was used to improve the early stages of hydration. The reference mixture design is shown in Figure 3. The secondary raw materials, WFS and WG, were added as a partial substitute for siliceous sand in amounts of 5 %, 10 %, and 15 %.

Properties	Units	Values
Initial set	min	168
Final set	min	236
Specific surface area	$cm^2\,g^{-1}$	5 730
Density	$kg\,m^{-3}$	3 120
Hydrating heat (7 days)	$J\,g^{-1}$	355

Table 4. Physical parameters CEM II/A-LL 52.5 R.

2.2. Sample preparation and treatment

The raw materials were weighed to the nearest gram, except for aluminium, which was weighed to the nearest microgram. The aerating agent was prepared by mixing the aluminium powder with lubricating soap (0.3 ml) in 75 ml of distilled water. The suspension prepared in this way was then stirred until the aluminium was completely dispersed in the water. Six mixtures were produced in which siliceous sand was partially replaced (at 5 %, 10 %, and 15 %) by a water suspension of secondary raw material. The amount of water contained in the suspension has been chosen to ensure the consistency of fresh mixtures remains constant. The dry ingredients, i.e. cement, lime, and gypsum, were added to the homogenised liquid ingredients in the container. All the components were mixed for 3 minutes. In the last stage of mixing, the aluminium powder was added in the form of a prepared suspension. The beaker containing the suspension was stirred for 1 minute on high speed. After the mixing, the suspension was dosed into moulds and cured in a laboratory climatic chamber at 40 °C for 24 hours. After the pre-hardening process of the samples, the autoclaving process took place. The autoclaving cycle was set to 10.5 hours, including isothermal endurance for 7 hours with a vapour pressure of 1.15 MPa.

2.3. Material testing

AAC is characterised by compressive strength expressed in $N\,mm^{-2}$ and bulk density expressed in $kg\,m^{-3}$. These two properties are dependent on each other. In general, the higher the bulk density of a material type, the higher its compressive strength [31]. In the production of aerated concrete, the aim is to achieve the highest possible strength while achieving the lowest possible bulk density, while the minimum declared compressive strength must be met and the maximum declared bulk density must not be exceeded [32].

Determining the dry mass of AAC was carried out according to EN 772-13 [33] as determined by EN 771-4+A1 [34]. However, the dry mass can also be de-

Oxides	Unit	REF	Foundry sand			Waste glass		
			WFS1	WFS2	WFS3	WG1	WG2	WG3
SiO_2	%	73.28	89.18	84.45	84.29	69.29	65.41	67.90
Al_2O_3	%	3.55	2.73	3.34	3.96	1.61	1.98	1.81
Fe_2O_3	%	1.05	1.02	1.53	2.07	0.61	1.07	1.14
CaO	%	0.33	0.17	0.52	0.45	11.24	10.53	10.99
MgO	%	0.16	0.03	0.55	0.39	1.30	2.00	1.53
Na_2O	%	0.62	0.45	0.53	0.46	13.16	12.57	13.13
K_2O	%	1.16	0.81	0.74	0.78	0.43	0.67	0.52
SO_3	%	0.05	0.04	0.01	0.02	0.11	0.00	0.03
TiO_2	%	0.16	0.05	0.11	0.25	0.07	0.10	0.08
MnO	%	0.04	0.01	0.02	0.02	0.02	0.03	0.04
P_2O_5	%	0.01	0.00	0.02	0.00	0.01	0.02	0.02

TABLE 5. Results of X-ray fluorescence analysis: chemical composition of raw materials expressed in oxides.

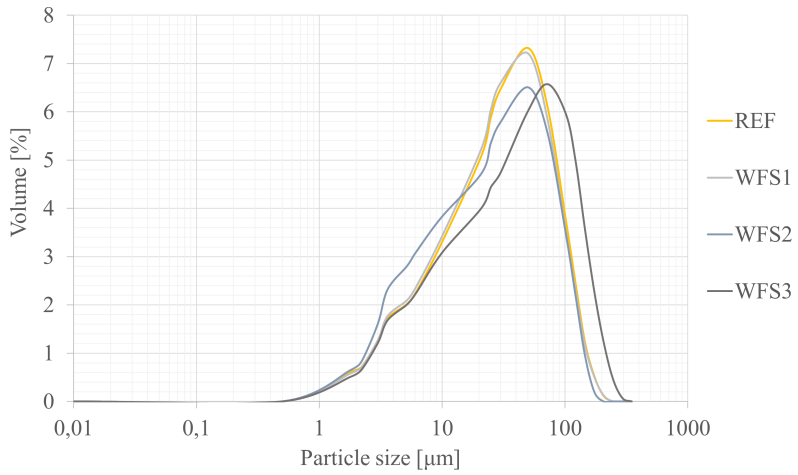

FIGURE 1. Comparison of particle size distribution of siliceous component based on waste foundry sand and reference siliceous sand.

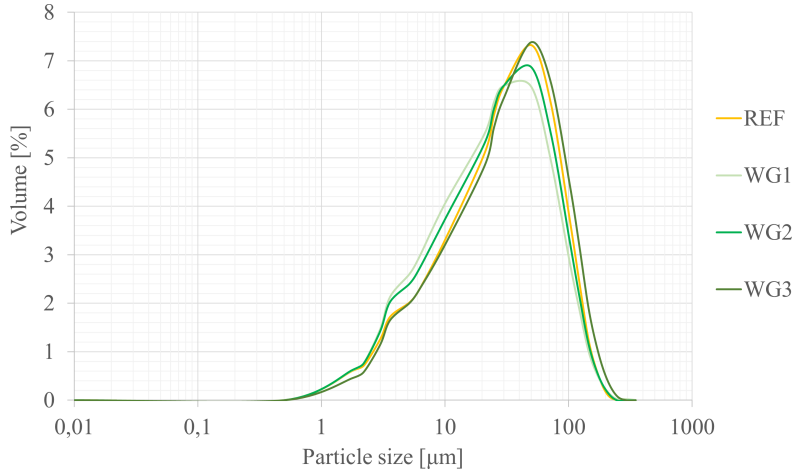

FIGURE 2. Comparison of particle size distribution of siliceous component based on waste glass and reference siliceous sand.

termined using EN 678 [35]. The principle of both tests is identical, but EN 678 [35] is adapted to the AAC technology, whereas EN 772-13 [33] describes the general procedure.

The compressive strength of the test specimens was determined according to EN 772-1+A1 [36] as determined by EN 771-4+A1 [34]. However, the compressive strength can also be determined according to EN 679 [37]. The principle of both tests is identical, but EN 679 [37] is adapted to the AAC technology, whereas EN 771-4+A1 [34] describes the general procedure.

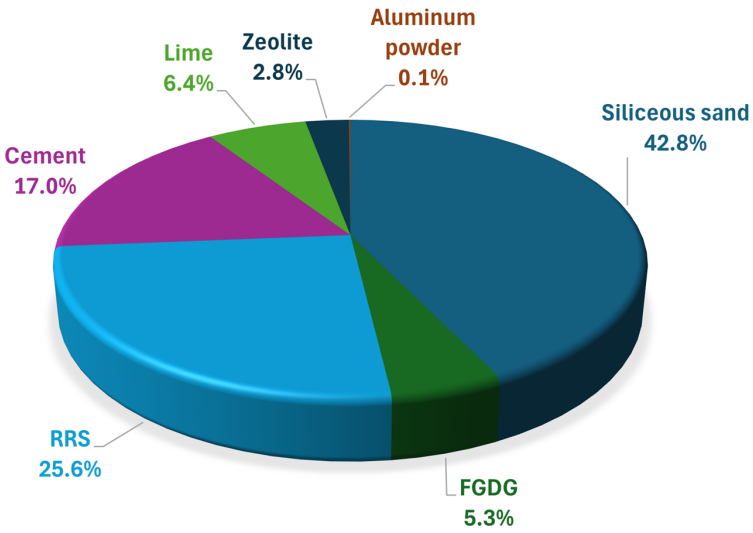

Figure 3. Reference AAC mixture.

The compressive strength and the bulk density of AAC (and also of other foamed and gas-silicates) can be correlated by means coefficient of the constructive quality (CCQ), which is calculated as follows: $\mathrm{CCQ} = \frac{f_c}{D_{\mathrm{dry}}} \cdot 100$ [-], where f_c is the compressive strength and D_{dry} is the dry bulk density [38]. It is an indicator of the interaction of the basic characteristics. It can be considered as a tool for an effective evaluation of results and serves as a quality indicator.

The mineralogical composition of the samples was determined using the Empyrean X-ray diffractometer from Malvern PanAnalytical. The results of the X-ray diffraction analysis were evaluated quantitatively using the Rietveld quantitative analysis. Calcium fluorite, as an inert standard, was added to the sample at an amount of 20 %. The monitored minerals and the amorphous component in the samples are calculated by the intensity of the isolated peaks compared to the peak intensity for calcium fluoride with HighScore measurement software.

3. Results and discussion

As the basic characteristics of AAC are dry bulk density and compressive strength, it was necessary to start the testing process with these properties.

The samples with 10 % replacement of foundry sand WFS1 and with 10 % replacement of mixed WG did not reach a bulk density of 450 kg m^{-3}. None of the samples exceeded the specified maximum bulk density (as seen in Figure 4). For the samples where silica sand was replaced with foundry sands WFS2 and WFS3, which originated from the production of iron castings, an increasing trend in bulk density was observed as the replacement dose of silica sand increased. However, for foundry sand WFS1, an initial decrease in bulk density was observed, followed by an increase. For the samples where silica sand was replaced with brown (WG2) or mixed waste glass (WG3), a slight initial decrease in bulk density was followed by a significant increase. The bulk density of the samples with pure WG increased steadily.

The compressive strength of most samples increased with increasing bulk density, but some samples deviated from this trend. For example, the samples containing 10 % of foundry sand WFS1, or WG2 replacements showed higher strength at lower bulk density.

The compressive strength of the specimens (Figure 5) showed an increasing trend with the replacement of silica sand with WFS2 foundry sand, but it was not enough to increase the bulk density. Conversely, the compressive strength of the samples with silica sand replaced by foundry sand WFS3 showed an increase with a relatively constant value of bulk density.

Samples containing foundry sand exhibited compressive strength values closely aligned with those of the reference sample. No substantial variations were observed, except for the WFS1 sample with a 10 % replacement, which slightly deviated.

The samples containing WG as a replacement for silica sand showed lower strengths than the reference sample. However, the sample with 15 % WG replacement bucked this trend, achieving higher values than the reference sample and significantly higher values than the other samples with WG replacement. The samples with a pure WG replacement achieved values of compressive strength that were lower, but still close to those of the reference samples.

The coefficient of the constructive quality (Figure 6) of the samples in which silica sand was replaced with foundry sand fluctuated closely around the values obtained for the reference sample. With the exception of the sample with 10 % of foundry sand, WFS1 did not show any significant fluctuations to higher or lower values.

The results of the basic testing of the physical and mechanical properties show that the samples with the highest percentage of silica sand replaced by each

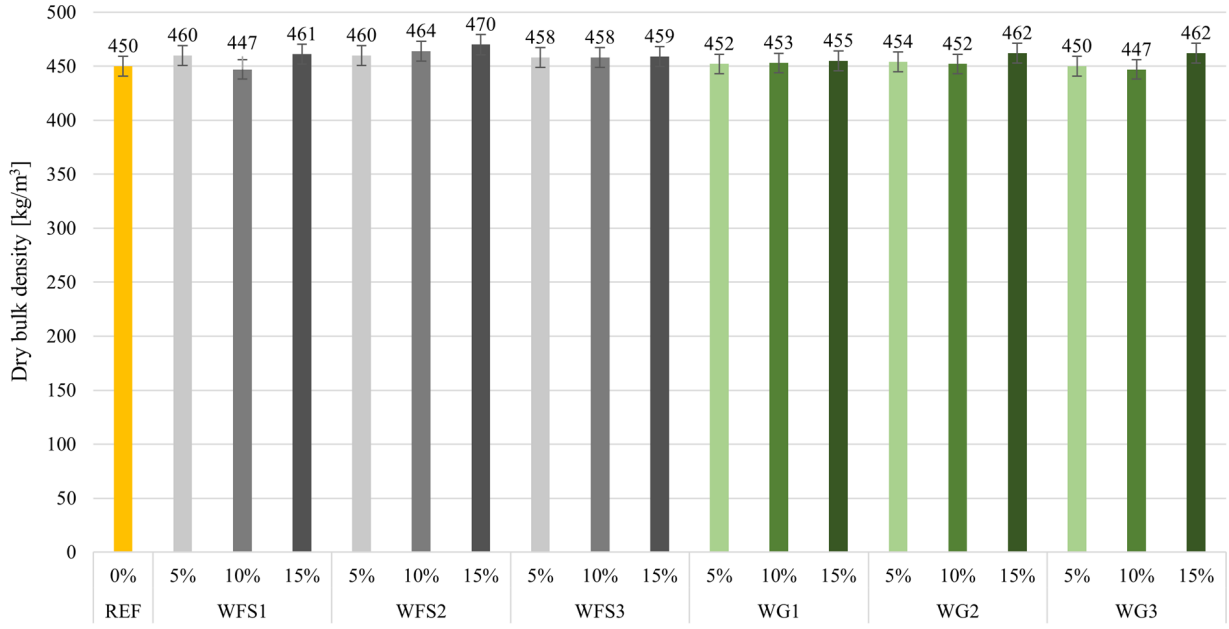

FIGURE 4. Dry bulk density.

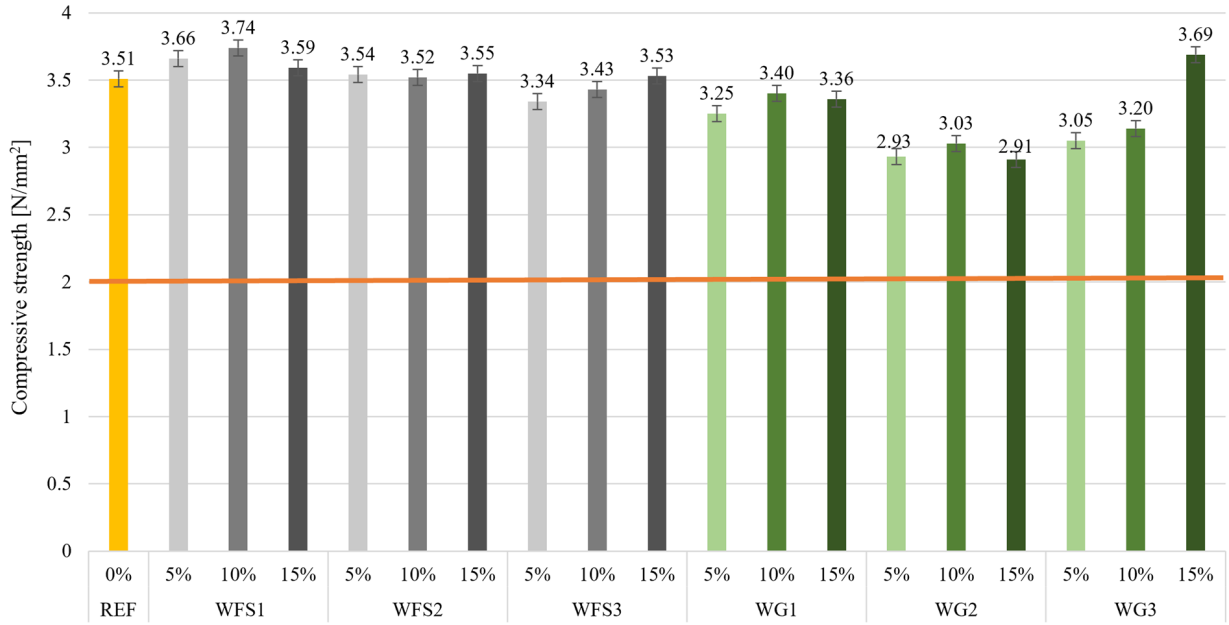

FIGURE 5. Compressive strength of all samples.

of the secondary raw materials used in this study did not differ significantly from those with lower replacement percentages, i.e. they showed very similar physical-mechanical properties. The exception was the sample with 15 % of waste mixed glass WG3, which significantly deviated from the samples with lower replacement percentages.

The values of the physical and mechanical properties of the samples with higher replacement percentages came out favourably and were not significantly different from those of the samples with lower replacement percentages.

The investigation of the mineral composition of the samples was carried out by an X-ray diffraction analysis, which was performed only qualitatively at this stage.

First, basic minerals commonly found in AAC were studied: quartz, tobermorite, alite, anhydrite, and calcite. Of particular importance is the occurrence and content of tobermorite.

Tobermorite crystallises in an orthorhombic structure, forming plate-like or sheet-like crystals. It is formed during the autoclaving process according to the following reaction: 3 $Ca(OH)_2$ + 2 SiO_2 (dissolved silica) → non-crystalline CSH + SiO_2 → $C_5S_6H_5$ (tobermorite) [39].

The addition of Al_2O_3 (used to lime the mass) to the system CaO-SiO_2-Al_2O_3-H_2O also produces hexagonal C_3AH_{12} (katoite) or C_4AH_{13}, which transforms into cubic C_3AH_6 [40].

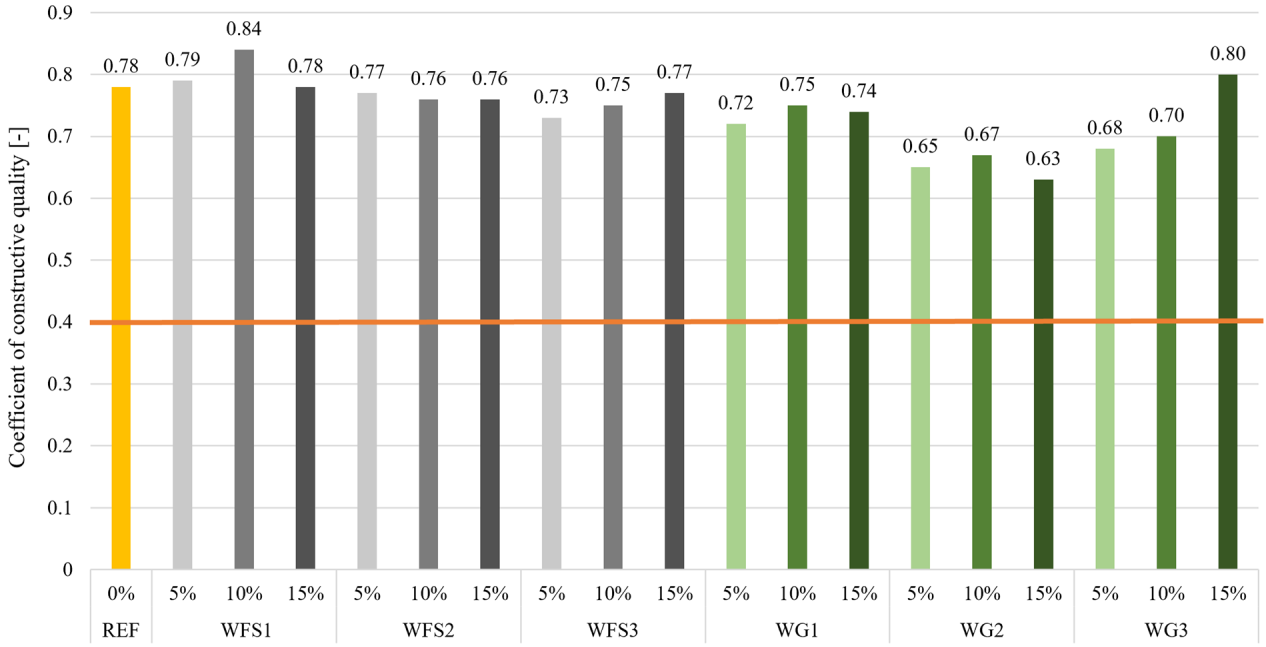

Figure 6. Coefficient of constructive quality values.

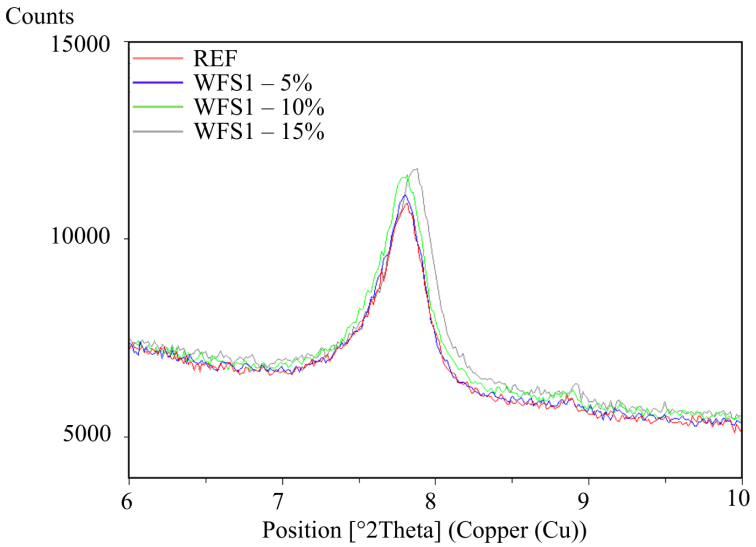

Figure 7. Change in peak intensity of 11 Å tobermorite at position 7.9° 2Theta for mixture with sand replaced by foundry sand WFS1.

Based on the above reaction, the amount of katoite ($Ca_3Al_2[(OH)_4]_3$), which crystallises in the square system, was also monitored [41]. This mineral forms when aluminium reacts with calcium hydroxide [42]. The amount of clinotobermorite was also monitored [43]. It is a mineral belonging to the group of tobermorites with the chemical formula $Ca_3(SiO_4)O$, crystallising in a monoclinic system [44].

Due to the increased Na_2O content in the WG, the occurrence and amount of albite in the structure was also monitored. Albite is a mineral belonging to the group of feldspars with the chemical formula NaAlSi3O8, crystallising in a ternary system [45].

In particular, the change in intensity of the most significant peak of 11 Å tobermorite at position 7.9° 2Theta was monitored. Since this 11 Å tobermorite peak is relatively isolated from other peaks for tobermorite and other minerals that are present in the AAC, a change in the amount of 11 Å tobermorite formed can be predicted from the change in its intensity.

For the samples in which silica sand was replaced by WFS (Figures 7–9), there was an increase in the peak intensity of 11 Å tobermorite at position 7.9 °2Theta compared to the reference sample, i.e. an increase in the amount of tobermorite in the samples with higher replacement percentages. The increase in intensity was mostly correlated with the replacement percentage. This phenomenon can be attributed to the fact that there was more silica dioxide present in all types of WFS than in the reference sand. Using different types of glass as a substitute for the silica component

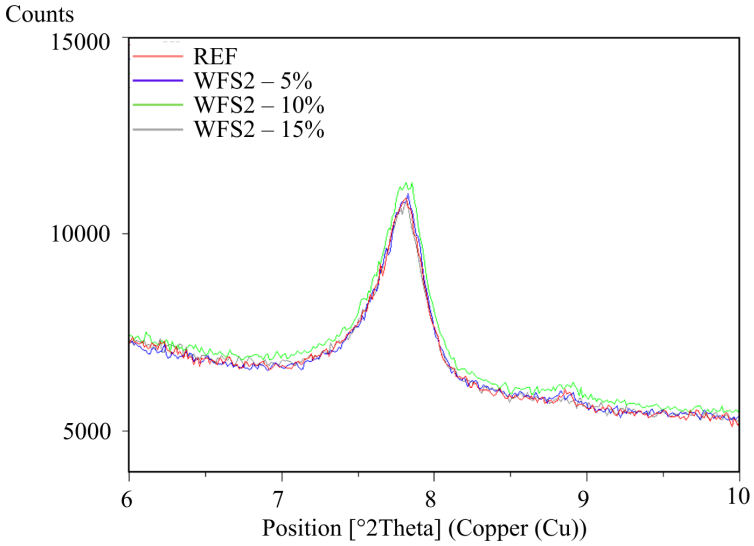

FIGURE 8. Change in peak intensity of 11 Å tobermorite at position 7.9° 2Theta for mixture with sand replaced by foundry sand WFS2.

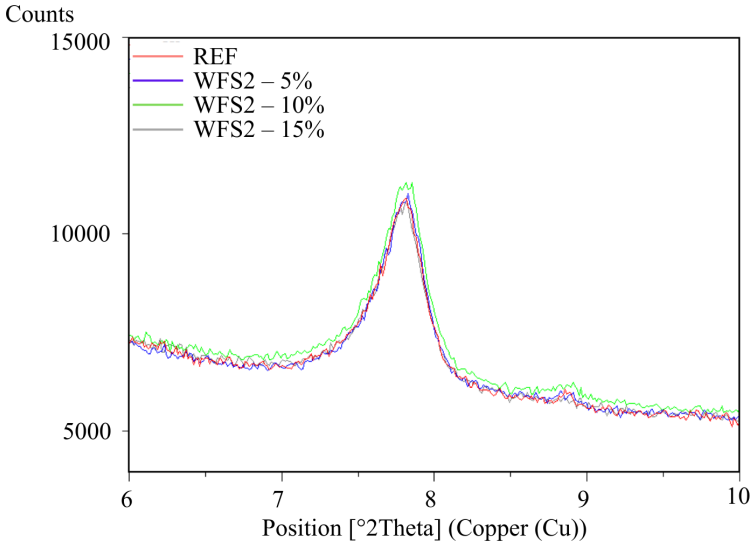

FIGURE 9. Change in peak intensity of 11 Å tobermorite at position 7.9° 2Theta for mixture with sand replaced by foundry sand WFS3.

in AAC can result in a change in microstructure [43]. The morphological changes may explain the changes in the behaviour of the samples with a higher content of WG. Slight fluctuations can be explained by statistical error, however, some samples deviated significantly from the trend in material behaviour.

In the case of the mixtures containing WG1, no significant change in the intensity of 11Å tobermorite at position 7.9° 2Theta, i.e. in its amount, was observed. The peaks for the mixtures with silica sand replaced by pure WG oscillate around the peak of the reference mixture (Figure 10).

In the case of the mixtures containing brown glass waste, a decrease in the intensity of 11 Å tobermorite at position 7.9° 2Theta, i.e. a decrease in its amount, could be observed, see Figure 11. The decrease was barely noticeable in the case of 5 % and 10 % replacements, and significant in the case of the 15 % replacement. This decrease for the 15 % replacement correlates with a slight decrease in compressive strength.

In the case of mixtures containing WG3 (Figure 12), a decrease in the intensity of 11 Å tobermorite at position 7.9° 2Theta, i.e. a decrease in its amount, could be observed. The decrease was minimal in the case of 5 % replacement, but more pronounced in the case of 10 % and 15 % replacements.

The results for the mixtures containing brown WG showed an anomalous behaviour – the decrease in the intensity of 11 Å tobermorite did not correspond with the trend in compressive strength. The sample with 5 % replacement had a peak intensity of 11 Å tobermorite very similar to that of the reference mixture, while the compressive strength was similar to the sample with a 15 % replacement, which in contrast had the lowest peak intensity of 11 Å tobermorite.

Another anomaly was the results for the samples

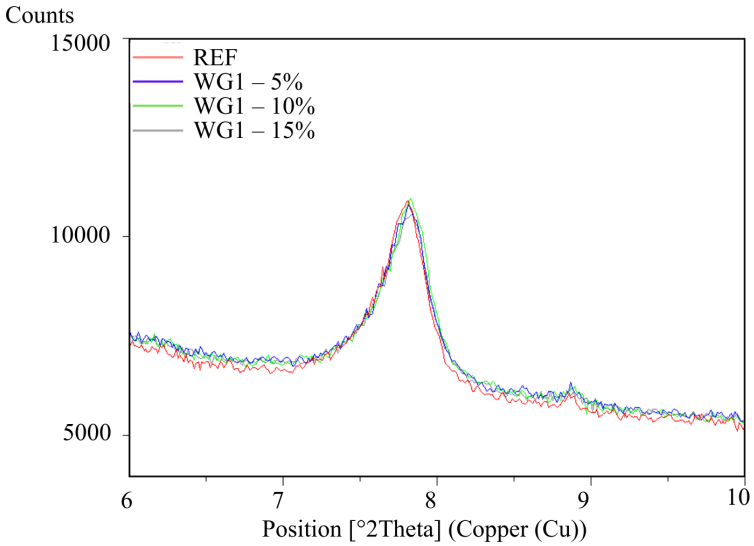

Figure 10. Change in peak intensity of 11 Å tobermorite at position 7.9° 2Theta for mixture with sand replaced by WG1.

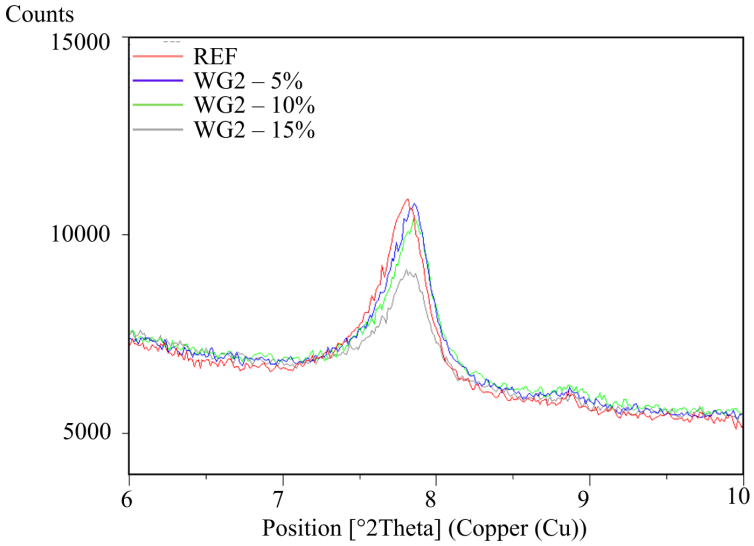

Figure 11. Change in peak intensity of 11 Å tobermorite at position 7.9° 2Theta for mixture with sand replaced by brown glass waste.

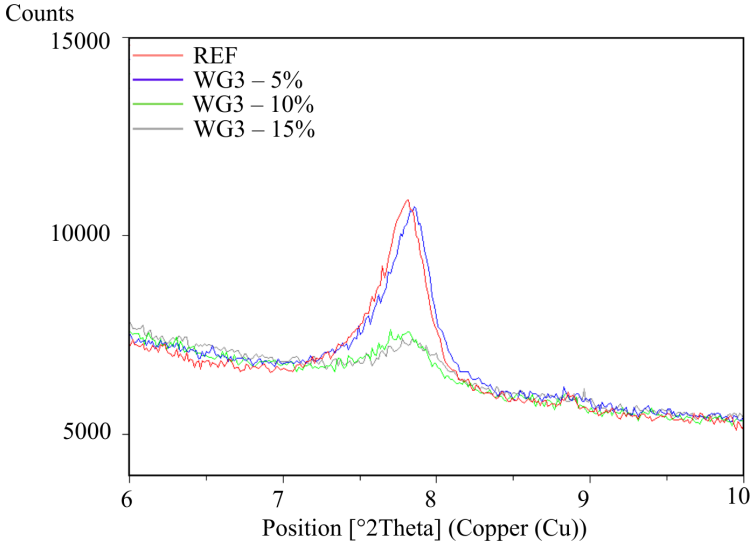

Figure 12. Change in peak intensity of 11Å tobermorite at position 7.9° 2Theta for mixture with sand replaced by WG3.

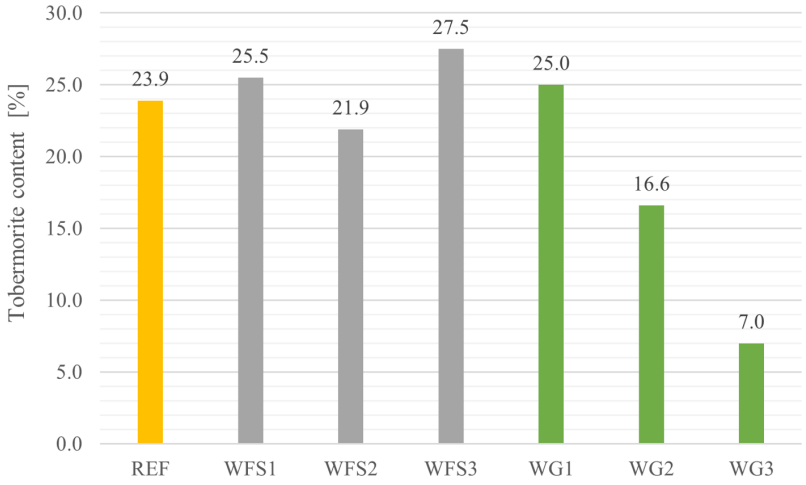

FIGURE 13. Comparison of tobermorite content in samples with 15 % of siliceous component replaced.

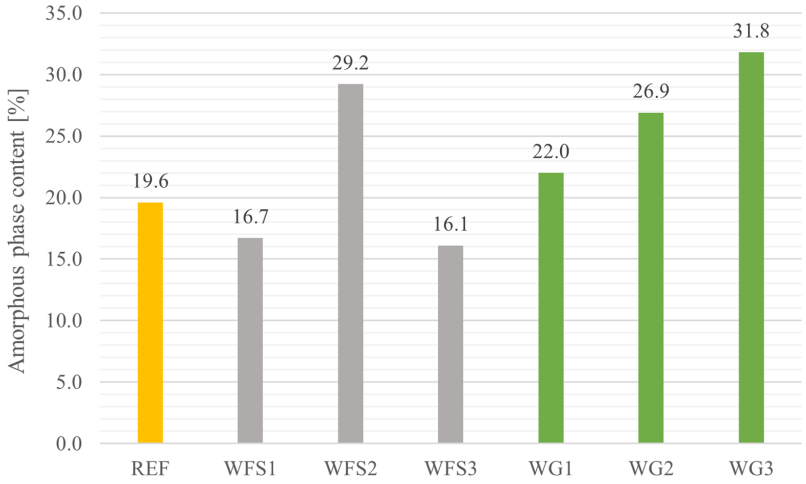

FIGURE 14. Comparison of amorphous phase content in samples with 15 % replacement of siliceous component.

containing mixed WG, where the intensity of the 11 Å tobermorite peak decreased significantly with increasing replacement percentage, but despite this, the strength increased. The sample with 15 % of silica sand replaced by WG showed the lowest peak intensity while exhibiting the highest strength of the set.

Following these findings, a quantitative Rietveld analysis focused mainly on tobermorite, and amorphous phase content was examined. Results are shown in Figures 13 and 14.

The results indicate that the WG2 and WG3 had a rapid influence on the decrease of tobermorite in the samples. This phenomenon is also associated with the increase in other mineral phases. The fine-milled amorphous glass present in the WG3 samples transformed into clinotobermorite, accounting for 8.4 % of the total sample. Clinotobermorite is structurally related to tobermorite 11 Å. The difference between these two minerals is the structural disorder of clinotobermorite, in which the infinite calcium polyhedral layers parallel to (001) are connected through double silicate chains [46]. The structure of the mineral is not only monoclinic as the structure of a normal tobermorite 11 Å, but also triclinic. This disorder results in a higher hardness of the clinotobermorite compared to tobermorite 11Å. Clinotobermorite formation is also connected with slightly higher amount of CaO in the chemical composition of the input raw material [47].

The decrease in tobermorite content is caused by the formation of another phase called katoite during the autoclaving process. Katoite is a crystalline form of C-A-S-H and is the primary hydration product formed during the autoclaving process [42]. The samples with WG2 and WG3 contained higher amount of anhydrite and calcite. They are created during the autoclaving process from monosulfoaluminate and ettringite phases, which are unstable during the autoclaving process [48].

4. Conclusion

The experimental investigation confirms that the partial replacement of silica sand with selected types of foundry sand and WG can be successfully implemented in the production of AAC without compromising its fundamental material properties. The studied substitutions at rates of 5 %, 10 %, and 15 % demonstrated favourable performance in terms of both dry

bulk density and compressive strength, with all samples exceeding the minimum quality requirements defined by the constructive quality coefficient thresholds. Among the tested secondary raw materials, the foundry sands WFS2 and WFS3, originating from ferrous casting processes, yielded stable and predictable behaviour with increasing substitution rates, maintaining strength while allowing a controlled rise in bulk density. Notably, the sample with 15 % mixed WG (WG3) substitution showed an improvement in compressive strength, surpassing even the reference sample. X-ray diffraction analyses confirmed the formation of key crystalline phases, primarily tobermorite, which remains the critical strength-contributing mineral in AAC. The presence of additional phases such as katoite points to complex hydration pathways introduced by the inclusion of alumina-rich secondary materials. Importantly, no detrimental mineral phases were detected that would suggest incompatibility or reactivity-related instability within the system. From a material engineering and sustainability perspective, the findings strongly support the possibility of incorporating industrial by-products and municipal waste-derived materials in AAC composition. In addition, significant economic and environmental benefits result from the reduction of the consumption of primary raw materials. Further research should focus on the long-term durability, life cycle assessment, and optimisation of curing conditions of incorporating waste materials into commercial AAC production.

List of symbols

AAC Autoclaved Aerated Concrete

FGD Flue-Gas Desulphurisation Gypsum

WG Sample with content of Waste Glass

WFS Sample with content of Waste Foundry Sand

REF Reference Sample

Acknowledgements

This paper was created with financial support from the Czech Science Foundation (GAČR), Standard project No. 23-04824S, "Influence of alternative raw material components on improvement of physico-mechanical properties of aerated autoclaved concrete".

References

[1] G. Stanescu, A. Badanoiu, A. Nicoara, G. Voicu. Brick and glass waste valorisation in the manufacture of aerated autoclaved concrete. *Revista de Chimie* **70**(3):828–834, 2019. https://doi.org/10.37358/rc.19.3.7015

[2] Y. L. Chen, J. E. Chang, Y. C. Lai, M. I. M. Chou. A comprehensive study on the production of autoclaved aerated concrete: Effects of silica-lime-cement composition and autoclaving conditions. *Construction and Building Materials* **153**:622–629, 2017. https://doi.org/10.1016/J.CONBUILDMAT.2017.07.116

[3] W. Mazur, Ł. Drobiec, R. Jasiński. Effects of specimen dimensions and shape on compressive strength of specific autoclaved aerated concrete. *CE/Papers* **2**(4):541–556, 2018. https://doi.org/10.1002/cepa.837

[4] Z. Owsiak, A. Sołtys, P. Sztąboroski, M. Mazur. Properties of autoclaved aerated concrete with halloysite under industrial conditions. *Procedia Engineering* **108**:214–219, 2015. https://doi.org/10.1016/J.PROENG.2015.06.140

[5] P. Walczak. Compressive strength of autoclaved aerated concrete: Test methods comparison. *CE/Papers* **2**(4):589–590, 2018. https://doi.org/10.1002/cepa.851

[6] A. Tawfik, R. A. Abd-El-Razik. Design, fabrication, and characterization of distinguished lightweight and sustainable building materials. *Journal of Building Engineering* **46**:103712, 2022. https://doi.org/10.1016/J.JOBE.2021.103712

[7] K. Matsui, J. Kikuma, M. Tsunashima, et al. In situ time-resolved X-ray diffraction of tobermorite formation in autoclaved aerated concrete: Influence of silica source reactivity and Al addition. *Cement and Concrete Research* **41**(5):510–519, 2011. https://doi.org/10.1016/j.cemconres.2011.01.022

[8] Abhilasha, R. Kumar, R. Lakhani, et al. Utilization of solid waste in the production of autoclaved aerated concrete and their effects on its physio-mechanical and microstructural properties: Alternative sources, characterization, and performance insights. *International Journal of Concrete Structures and Materials* **17**(1):6, 2023. https://doi.org/10.1186/s40069-022-00569-x

[9] A. Raj, A. C. Borsaikia, U. S. Dixit. Manufacturing of autoclaved aerated concrete (AAC): Present status and future trends. In M. S. Shunmugam, M. Kanthababu (eds.), *Advances in Simulation, Product Design and Development*, pp. 825–833. Springer Singapore, Singapore, 2020. https://doi.org/10.1007/978-981-32-9487-5_69

[10] R. A. Rahman, A. Fazlizan, N. Asim, A. Thongtha. A review on the utilization of waste material for autoclaved aerated concrete production. *Journal of Renewable Materials* **9**(1):61–72, 2021. https://doi.org/10.32604/jrm.2021.013296

[11] W. Feng, Z. Li, Q. Long, et al. Study on the properties of autoclaved aerated concrete with high content concrete slurry waste. *Developments in the Built Environment* **17**:100338, 2024. https://doi.org/10.1016/j.dibe.2024.100338

[12] S. Seifert, A.-L. Liesch, V. Thome, et al. Application of recycled waste material for the production of autoclaved aerated concrete. *CE/Papers* **2**(4):495–502, 2018. https://doi.org/10.1002/cepa.867

[13] A. Różycka, Ł. Kotwica. Waste originating from the cleaning of flue gases from the combustion of industrial wastes as a lime partial replacement in autoclaved aerated concrete. *Materials* **15**(7):2576, 2022. https://doi.org/10.3390/ma15072576

[14] A. Mohammadi, E. Ghiasvand, M. Nili. Relation between mechanical properties of concrete and alkali-silica reaction (ASR): A review. *Construction and Building Materials* **258**:119567, 2020. https://doi.org/10.1016/j.conbuildmat.2020.119567

[15] I. A. Manaf, N. Marsi, E. Yusrianto, et al. Evaluation of physical properties of autoclaved aerated concrete (AAC) based glass-gypsum waste into concrete. *Malaysian Journal of Chemical Engineering & Technology* **5**(1):1–7, 2022. https://doi.org/10.24191/mjcet.v5i1.14774

[16] N. Kızılkaya, D. Eren Sarıcı. Preparation and performance comparison of autoclaved aerated concrete by using ceramic and glass wastes instead of silica. *Dicle University Journal of Engineering* **15**(2):463–479, 2024. https://doi.org/10.24012/dumf.1422548

[17] W. Chen, D. Liu, Y. Liang. Influence of ultra fine glass powder on the properties and microstructure of mortars. *Fluid Dynamics & Materials Processing* **20**(5):915–938, 2024. https://doi.org/10.32604/FDMP.2024.046335

[18] Český statistický úřad. Produkce, využití a odstranění odpadů – 2021 [In Czech; Generation, recovery and disposal of waste – 2021], 2022. [2025-02-03]. https://www.czso.cz/csu/czso/produkce-vyuziti-a-odstraneni-odpadu-mgyqmwjyr8

[19] L. Mészárosová, V. Černý, J. Melichar, R. Drochytka. Effect of alternative fibre-like secondary raw materials utilization by the preparation of the aerated autoclaved concrete. *CE/Papers* **6**(2):430–436, 2023. https://doi.org/10.1002/cepa.2088

[20] A. Laukaitis, J. Kerienė, D. Mikulskis, et al. Influence of fibrous additives on properties of aerated autoclaved concrete forming mixtures and strength characteristics of products. *Construction and Building Materials* **23**(9):3034–3042, 2009. https://doi.org/10.1016/j.conbuildmat.2009.04.007

[21] M. Arun Kumar, K. Prasanna, C. Chinna Raj, et al. Bond strength of autoclaved aerated concrete manufactured using partial replacement of flyash with fibers – A review. *Materials Today: Proceedings* **65**:581–589, 2022. https://doi.org/10.1016/j.matpr.2022.03.191

[22] S. Klepek, S. Jonášová. Waste as a resource, 2017. https://zajimej.se/odpad-jako-zdroj-jak-vypada-odpadove-hospodarstvi-ve-slevarenske-vyrobe/

[23] Zajimej.se. Odpad jako zdroj: Jak vypadá odpadové hospodářství ve slévárenské výrobě? [In Czech; Forming mixtures from foundries], 2023. [2025-02-03]. https://odpady-online.cz/formovaci-smesi-ze-slevaren/

[24] D. Sangavi, K. A. Senthil. Utilisation of foundry sand in concrete – A review. *International Research Journal of Multidisciplinary Technovation* **1**(6):383–386, 2019. https://doi.org/10.34256/irjmtcon51

[25] J. Ahmad, Z. Zhou, R. Martínez-García, et al. Waste foundry sand in concrete production instead of natural river sand: A review. *Materials* **15**(7):2365, 2022. https://doi.org/10.3390/ma15072365

[26] K. Smit, A. Nakum, A. Bhogayata. Use of used foundry sand in concrete: A state of art review. *International Journal of Research in Engineering and Technology* **3**(2):586–589, 2014.

[27] B. Bhardwaj, P. Kumar. Waste foundry sand in concrete: A review. *Construction and Building Materials* **156**:661–674, 2017. https://doi.org/10.1016/J.CONBUILDMAT.2017.09.010

[28] M. Selvakumar, S. Geetha, S. M. Lakshmi. Investigation on properties of aerated concrete with foundry sand as replacement for fine aggregate. *Materials Today: Proceedings* **65**:1666–1673, 2022. https://doi.org/10.1016/J.MATPR.2022.04.709

[29] Vyhláška č. 8/2021 Sb.: Vyhláška o Katalogu odpadů a posuzování vlastností odpadů (Katalog odpadů) [In Czech; Decree No. 8/2021 coll.: On the waste catalogue and the assessment of waste properties (Waste catalogue)], 2021. https://www.zakonyprolidi.cz/cs/2021-8

[30] European Committee for Standardization. EN 459-1: Building lime – Part 1: Definitions, specifications and conformity criteria, 2015.

[31] E. Michelini, D. Ferretti, L. Miccoli, F. Parisi. Autoclaved aerated concrete masonry for energy efficient buildings: State of the art and future developments. *Construction and Building Materials* **402**:132996, 2023. https://doi.org/10.1016/J.CONBUILDMAT.2023.132996

[32] K.-H. Yang, K.-H. Lee. Tests on high-performance aerated concrete with a lower density. *Construction and Building Materials* **74**:109–117, 2015. https://doi.org/10.1016/J.CONBUILDMAT.2014.10.030

[33] European Committee for Standardization. EN 772-13: Methods of test for masonry units – Part 13: Determination of net and gross dry density of masonry units (except natural stone), 2000.

[34] European Committee for Standardization. EN 771-4: Specification for masonry units – Part 4: Autoclaved aerated concrete masonry units, 2011. Corrigendum/Amendment 1: 2015.

[35] European Committee for Standardization. EN 678: Determination of the dry density of autoclaved aerated concrete, 1993.

[36] European Committee for Standardization. EN 772-1: Methods of test for masonry units – Part 1: Determination of compressive strength, 2011.

[37] European Committee for Standardization. EN 679: Determination of the compressive strength of autoclaved aerated concrete, 2005.

[38] Y. O. Özkılıç', A. N. Beskopylny, S. A. Stel'makh, et al. Lightweight expanded-clay fiber concrete with improved characteristics reinforced with short natural fibers. *Case Studies in Construction Materials* **19**:e02367, 2023. https://doi.org/10.1016/j.cscm.2023.e02367

[39] T. Shams, G. Schober, D. Heinz, S. Seifert. Production of autoclaved aerated concrete with silica raw materials of a higher solubility than quartz Part II: Influence of autoclaving temperature. *Construction and Building Materials* **287**:123072, 2021. https://doi.org/10.1016/j.conbuildmat.2021.123072

[40] B. Lothenbach, D. Jansen, Y. Yan, J. Schreiner. Solubility and characterization of 11 Å Al-tobermorite. *Cement and Concrete Research* **159**:106871, 2022. https://doi.org/10.1016/J.CEMCONRES.2022.106871

[41] K. Mesecke, W. Malorny, L. N. Warr. Understanding the effect of sulfate ions on the hydrothermal curing of autoclaved aerated concrete. *Cement and Concrete Research* **164**:107044, 2023. https://doi.org/10.1016/j.cemconres.2022.107044

[42] S. Kanehira, S. Kanamori, K. Nagashima, et al. Controllable hydrogen release via aluminum powder corrosion in calcium hydroxide solutions. *Journal of Asian Ceramic Societies* **1**(3):296–303, 2013. https://doi.org/10.1016/j.jascer.2013.08.001

[43] P. Walczak, J. Małolepszy, M. Reben, et al. Utilization of waste glass in autoclaved aerated concrete. *Procedia Engineering* **122**:302–309, 2015. https://doi.org/10.1016/j.proeng.2015.10.040

[44] T. Maeshima, H. Noma, M. Sakiyama, T. Mitsuda. Natural 1.1 and 1.4 nm tobermorites from Fuka, Okayama, Japan: Chemical analysis, cell dimensions, ^{29}Si NMR and thermal behavior. *Cement and Concrete Research* **33**(10):1515–1523, 2003. https://doi.org/10.1016/S0008-8846(03)00099-1

[45] L. Cai, T. Tang, M. Liu, D. Xie. Comparative study of carbide slag autoclaved aerated concrete (AAC) manufactured under thermal oven and microwave precuring process: Foaming course, rough body strength and physic-mechanical properties. *Construction and Building Materials* **236**:117550, 2020. https://doi.org/10.1016/j.conbuildmat.2019.117550

[46] S. Merlino, E. Bonaccorsi, T. Armbruster. The real structures of clinotobermorite and tobermorite 9 Å: OD character, polytypes, and structural relationships. *European Journal of Mineralogy* **12**(2):411–429, 2000. https://doi.org/10.1127/0935-1221/2000/0012-0411

[47] K. Matsuo. *Thermodynamic modeling of the $CaO-SiO_2-H_2O$ cementitious system & the production of waste derived cement.* Master's thesis, McGill University, Department of Mining and Materials Engineering, 2017. https://doi.org/10.13140/RG.2.2.31692.56969

[48] G. V. P. Bhagath Singh, K. L. Scrivener. Investigation of phase formation, microstructure and mechanical properties of LC^3 based autoclaved aerated blocks. *Construction and Building Materials* **344**:128198, 2022. https://doi.org/10.1016/j.conbuildmat.2022.128198